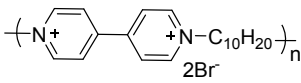
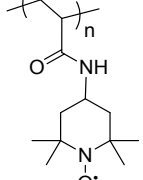
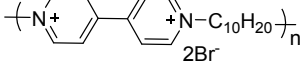
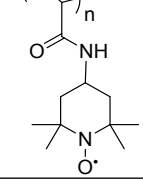
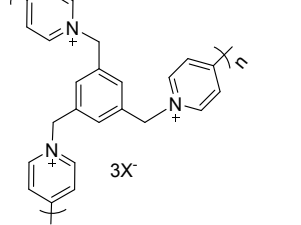
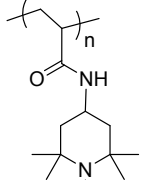
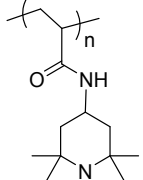


Supplementary Information

High-Performance All-Organic Aqueous Battery Based on Poly(imide) Anode and Poly(catechol) Cathode

Nagaraj Patil*^[a], Andreas Mavrandonakis^[a], Christine Jérôme^[b], Christophe Detrembleur^[b], Nerea Casado^[c], David Mecerreyes^[c,d], Jesus Palma^[a], and Rebeca Marcilla*^[a]

Table S1. Comparison of PI–PC full-cell performance metrics with the state-of-the-art all-organic aqueous stationary batteries

#[REF]	organic anode	organic cathode	charge carrier	electrolyte	output voltage (V)	cycling performance: retention; cycles; C-rate or current density	rate performance: C _s ; C _s retention; (C-rate or current density)
p – p type							
1 ¹			BF ₄ ⁻ -ion	0.1 M NaBF ₄	1.2	80% 2000 60C	104 ^a (60C)
2 ²			BF ₄ ⁻ -ion	1 M NaBF ₄	1.2	~75% 500 10C	~95 ^a (10C)
3 ³			Cl ⁻ -ion	0.1 M NaCl	1.3	80% 2000 10.5A/g	165 ^b , 100% (120C) 140 ^b , 85% (240C) 110 ^b , 63% (1200C)
n – p type							
4 ⁴	anthraquinone-derived poly(ethyleneimine)		Na ⁺ and Cl ⁻ -dual ion	0.1 M NaCl	1.2	>90% 60 0.04 mA/cm ²	60 ^a (18C)

5 ²	anthraquinone-derived poly(ethyleneimine)		Na ⁺ and Cl ⁻ - dual ion	3 M NaCl	1.1	~80% 100 10C	84 ^a (10C)
6 ⁵			Li ⁺ and TFSI ⁻ - dual ion	21m LiTFSI	1	85% 700 0.5A/g	105 ^a , 100% (0.5 A/g) 74 ^a , 70% (10 A/g) 48 ^a , 46% (50 A/g)
7 ⁶			NH ₄ ⁺ and SO ₄ ⁻ - dual ion	1 M (NH ₄) ₂ SO ₄	1.25	86.4% 10000 5A/g	137 ^b , 100% (0.5 A/g) 80 ^b , 58% (10 A/g) 25 ^b , 18% (50 A/g)
8 ⁷			Na ⁺ and ClO ₄ ⁻ - dual ion	NaClO ₄ -PVA	1.06	~55% 50 100 mV/s	152 ^b , 100% (1 A/g) 80 ^b , 52% (3 A/g) 63 ^b , 41% (5 A/g)
n – n type							
9 This work			Li ⁺ -ion	2.5 M LiNO ₃	0.6	80% 1000 5A/g	155 ^b , 100% (0.5 A/g) 118 ^b , 76% (120 A/g) 48 ^b , 23% (500 A/g)
10 This work			Zn ²⁺ -ion	2.5 M ZnSO ₄	0.72	74% 1000 5A/g	147 ^b , 100% (0.5 A/g) 43 ^b , 76% (120 A/g) 7 ^b , 29% (250 A/g)
11 This work			Al ³⁺ -ion	2.5 M Al(NO ₃) ₃	0.9	53% 1000 5A/g	134 ^b , 100% (0.5 A/g) 83 ^b , 62% (10 A/g) 7 ^b , 6% (60 A/g)
12 This work			Li ⁺ and H ⁺ -hybrid ion	2.5 M Li ₂ SO ₄ and 0.25 M H ₂ SO ₄	0.95	75% 1000 5A/g	149 ^b , 100% (0.5 A/g) 90 ^b , 60% (120 A/g) 17 ^b , 12% (500 A/g)
13 ⁸	anthraquinone substituted PEDOT	benzoquinone substituted PEDOT	H ⁺ -ion	0.1 M 2-fluoropyridine	0.5	80% 150 3C	103 ^b , 100% (0.5C) 90 ^b , 83% (3C) 25 ^b , 74% (160C)
14 ⁹		PEDOT-lignin	Na ⁺ and H ⁺ -hybrid ion	1 M Na ₂ SO ₄ and 0.1 M HClO ₄	0.95	85% 800 100C	53 ^b , 100% (10C) 44 ^b , 83% (50C) 39 ^b , 74% (200C)

15 ¹⁰	<chem>*N1C(=O)c2cc(C(=O)N(C*)c3cc(*)c4c(c3)N(*)C(=O)c4=O)cc2C1=O</chem>	<chem>*Nc1ccc(cc1)[S+]([Cl])c2ccc(cc2)N(*)</chem>	NH ₄ ⁺ and H ⁺ -hybrid ion	1 M (NH ₄) ₂ SO ₄ and 1 M H ₂ SO ₄	0.75	80% 10000 5A/g	169 ^b , 100% (1 A/g) 105 ^b , 62% (5 A/g) 76 ^b , 45% (10 A/g)
------------------	---	---	---	--	------	----------------------	--

Specific capacities are expressed in mAh g⁻¹, either based on cathode-active material^a or anode-active material^b. nC-rate designates that the current chosen will charge/discharge the battery in 1/n hour.

Electrolyte salts: sodium tetrafluoroborate (NaBF₄), sodium chloride (NaCl), lithium bis(trifluoromethanesulfonyl)imide (LiTFSI), ammonium sulfate ((NH₄)₂SO₄), sodium perchlorate (NaClO₄), sodium sulfate (Na₂SO₄), perchloric acid (HClO₄), sulfuric acid (H₂SO₄), lithium sulfate (Li₂SO₄), zinc sulfate (ZnSO₄), aluminium sulfate (Al₂(SO₄)₃).

PVA: poly(vinyl alcohol).

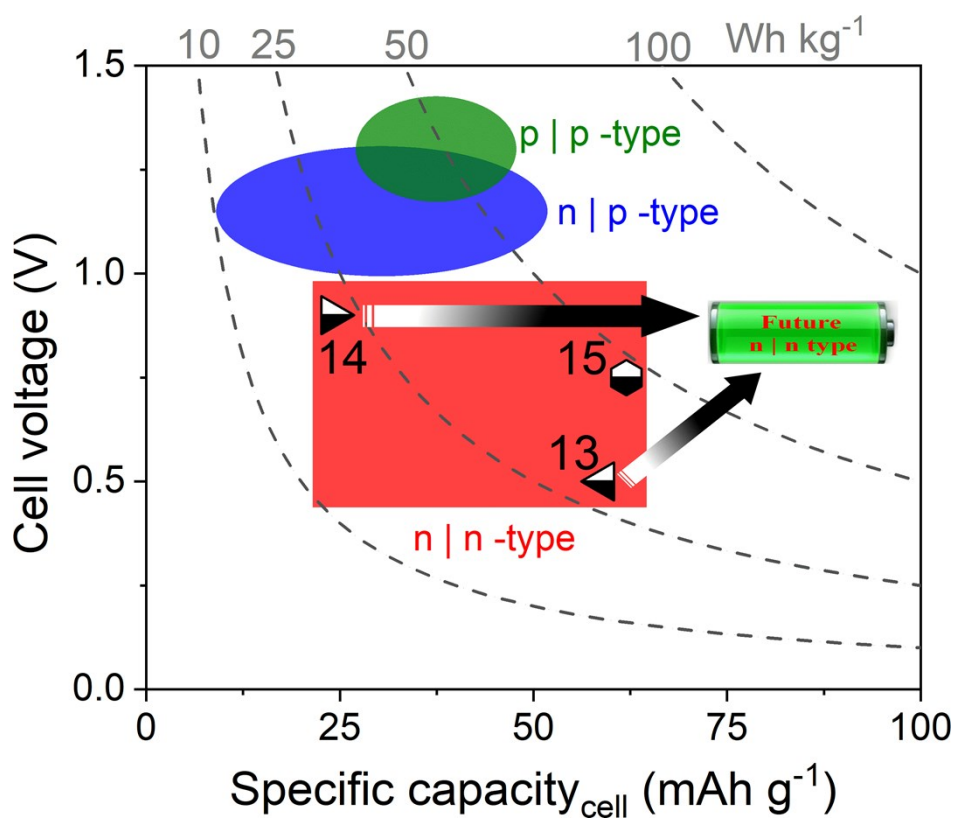


Figure S1. Cell voltage vs specific capacity of the reported all-polymer aqueous stationary batteries. The specific capacity is evaluated based on the total mass of the anode, cathode and consumed salt (charge carriers in the electrolyte). This plot for various aqueous all-organic full-cells (mostly, all-polymer) is computed by considering some of the best performing full-cells in their class (see Table S1). Light green, blue and red regions represent p/p, n/p, and n/n-type combinations, respectively. Symbols 13, 14 and 15 correspond to the entries 13, 14 and 15, respectively, in Table 1.

Computational Procedure

The structure of the PI/PC polymer is truncated to a simple monomer structure that is composed by a naphthalenetetracarboxylic diimide (NDI) unit with a $-CH_3$ group at the nitrogen position and a catecholate (CAT) moiety respectively. Since we are interested in the relative trends upon binding with various cations, reducing the size of the polymer to a NDI/CAT moiety will not change the conclusions for the cation insertion in the PI/PC polymers. We followed the same computational approach as described in our previous work.¹¹ The geometries of all structures are optimized with the local meta-GGA M06-L¹² in combination with the 6-31+G(d,p) basis set for non-metal atoms and the def2-SVP for metal cations. All basis sets have been obtained from the Basis Set Exchange library.¹³ The structures are verified to be minima after performing a frequency analysis, where no imaginary frequencies are computed. Final electronic energies are calculated using the M06-2X functional in combination with the 6-311++G(d,p) basis set for non-metals and the def2-TZVP for metal cations. All calculations (geometry optimizations, frequency calculations and final single point energies) are carried out in aqueous phase with the solvent treated by the implicit universal solvation model SMD.¹⁴ Free energies are calculated assuming $T = 298.15\text{ K}$ and $P = 1\text{ atm}$, based on the quantum mechanical harmonic-oscillator approximation from the vibrational partition functions. All calculations have been performed utilizing the Gaussian 16 package.¹⁵

Binding energies and redox potentials of PI are calculated for the formation of complexes between the NDI and Li^+ , Zn^{2+} and Al^{3+} metal cations that are considered to have their first coordination sphere filled with explicit water molecules. The corresponding binding energies and redox potentials for the cathode counterpart (catechol polymer, PC) are taken from our previous publication.¹¹ In the case of monovalent cations, we consider binding of the $[NDI]^{2-}$ dianion with two solvated cations, whereas for the di- and tri-valent cations binding with only one cation is considered. When a trivalent cation is bound, the total charge of the complex is considered to be +1. The overall reaction considered is shown in (1):



Initially, the most stable positions for the binding of lithium cations with the NDI dianion have been identified, by considering all possible combinations of placing the solvated lithium cations around the oxygen

atoms. The results are summarized in Figure S2. We identified several close-lying conformations that differ by less than 2.0 kcal/mol, which is converted to a difference of only 0.03 V in their reduction potentials. The most stable conformation is when the solvated lithium cations occupy the trans positions. Based on this, we considered only one conformation for rest of the cations.

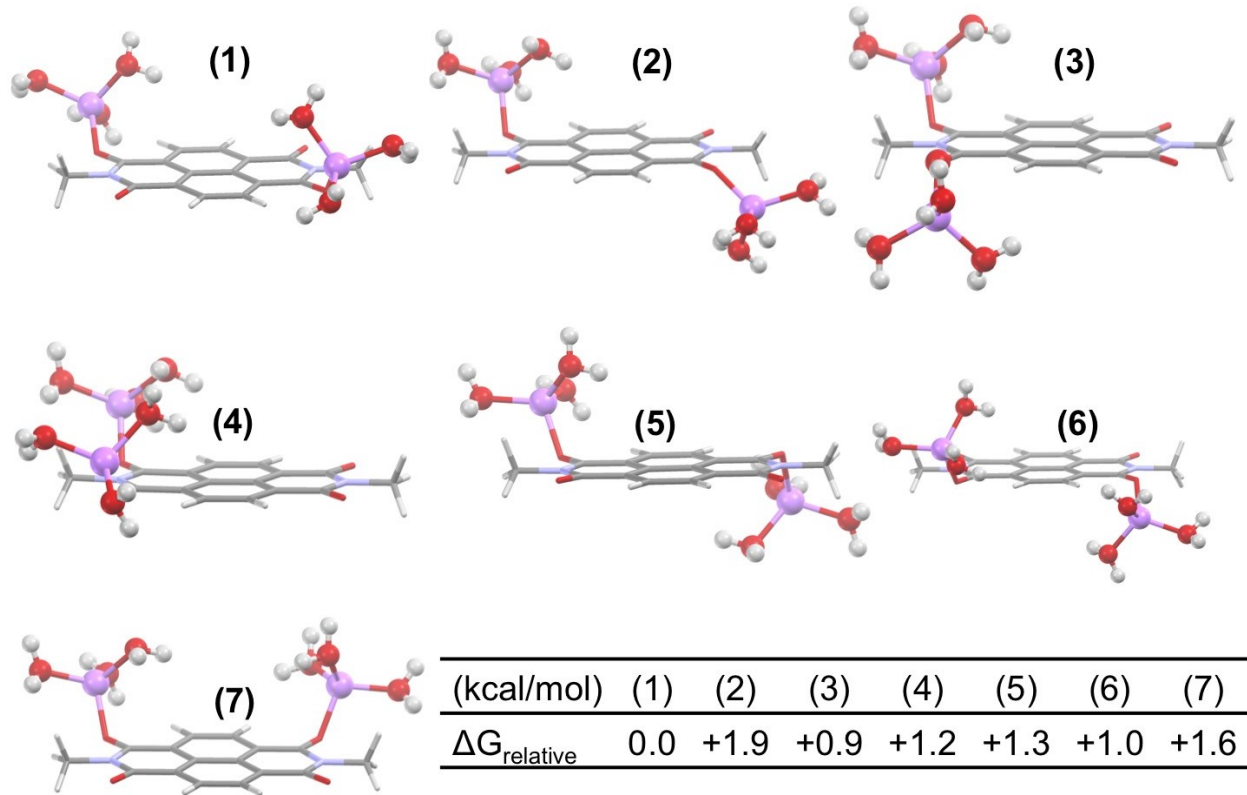


Figure S2. Electronic structures of the most stable conformations of solvated lithium cations with the NDI. Their relative free energies (in kcal/mol) are also reported.

The structures of $\text{NDI}^{2-}(\text{mM}^{\text{n}+})$ complexes are presented in the following Figure S3. For Al^{3+} , two possibilities have been studied. It can bind as an $\text{Al}(\text{H}_2\text{O})_6^{3+}$ or as $\text{Al}(\text{H}_2\text{O})_5(\text{OH})^{2+}$ with the NDI^{2-} . However, the difference in binding energy and absolute reduction potentials were less than 0.1 kcal/mol and 5 mV, respectively, between them.

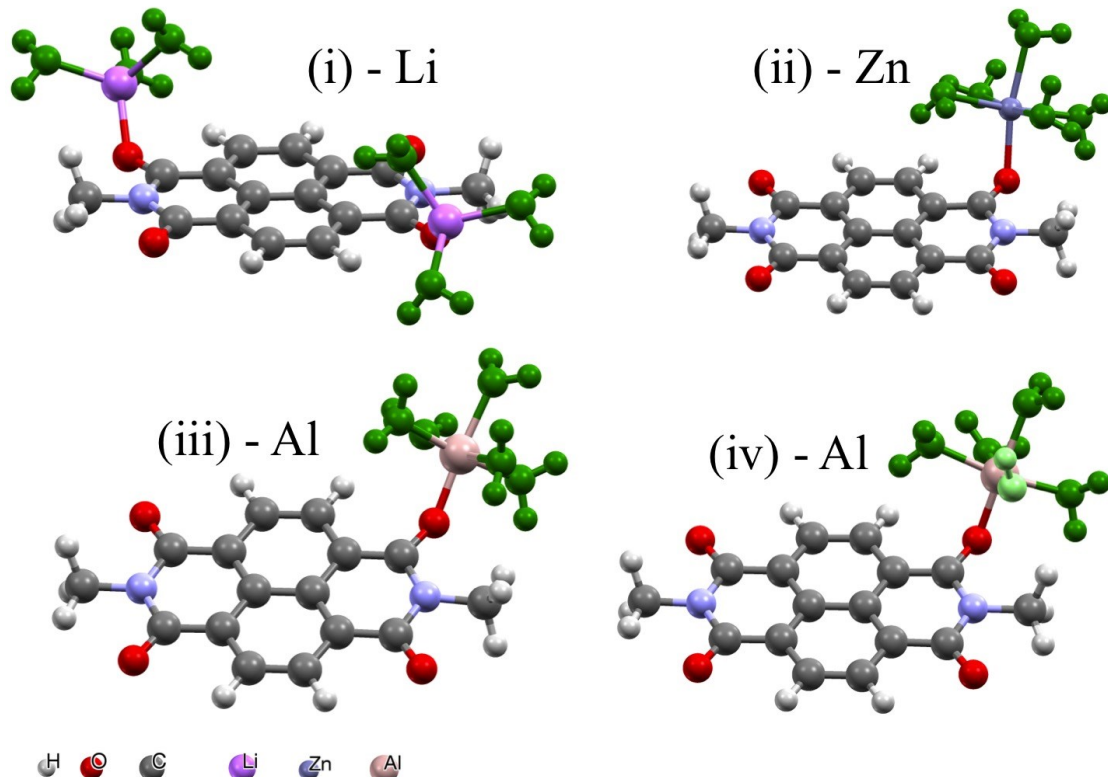


Figure S3. Electronic structures of the complexes between hydrated metal cations and the reduced NDI^{2-} . i) 2 Li^+ with 6 Aqua ligands, ii) 1 Zn^{2+} with 5 Aqua ligands, iii) 1 Al^{3+} with 5 Aqua ligands, and viii) 1 Al^{3+} with 1 OH and 4 Aqua ligands. The Aqua ligands are shown in green colour and the –OH ligand with light green.

Cartesian coordinates for the computed species

NDI $^{2-}$				NDI $^{2-}[\text{Li}(\text{H}_2\text{O})_4]^+$			
O	-3.5397	2.3115	1E-6	O	-1.48076	-3.90183	-0.56545
N	-3.48517	0.00356	0	N	-2.80538	-2.01284	-0.55508
O	-3.55345	-2.28728	-1E-6	O	-4.21897	-0.21666	-0.57717
C	-1.41667	1.23873	0	C	-0.40689	-1.77849	-0.54609
C	-0.68318	2.46587	1E-6	C	0.9119	-2.32925	-0.54712
C	-0.68327	-2.46251	-1E-6	C	-2.01826	1.63228	-0.54951
C	-1.4143	-1.2345	0	C	-1.87503	0.21004	-0.55083
C	-0.7186	0.00265	0	C	-0.57946	-0.3714	-0.53751
C	-2.84412	1.2541	0	C	-1.54642	-2.64052	-0.55745
C	-2.84035	-1.2406	-1E-6	C	-3.01666	-0.63552	-0.56106
H	-1.23579	3.40126	1E-6	H	1.02439	-3.40931	-0.56864
H	-1.23722	-3.39724	-1E-6	H	-3.0189	2.05614	-0.56805
O	3.55345	-2.28728	-1E-6	O	1.49197	4.00775	-0.47817
N	3.48517	0.00356	0	N	2.79836	2.12592	-0.4548
O	3.5397	2.3115	1E-6	O	4.21383	0.3105	-0.43529
C	1.4143	-1.2345	0	C	0.39709	1.8904	-0.50796
C	0.68327	-2.46251	-1E-6	C	-0.91988	2.44411	-0.5278
C	0.68318	2.46587	1E-6	C	2.01041	-1.51725	-0.52709
C	1.41667	1.23873	1E-6	C	1.8711	-0.09412	-0.49996
C	0.7186	0.00265	0	C	0.57364	0.48424	-0.51543
C	2.84035	-1.2406	0	C	1.53969	2.74487	-0.48218
C	2.84412	1.2541	0	C	3.01856	0.74597	-0.45986
H	1.23722	-3.39724	-1E-6	H	-1.02966	3.52475	-0.52638
H	1.23579	3.40126	1E-6	H	3.00933	-1.94495	-0.53959
C	4.94097	-0.03675	0	C	3.94412	3.02574	-0.41333
H	5.31675	0.98252	3E-6	H	4.8537	2.43404	-0.36986
H	5.30704	-0.56354	-0.88397	H	3.88246	3.6726	0.46397
H	5.30704	-0.56355	0.88397	H	3.95963	3.65979	-1.30237
C	-4.94097	-0.03675	0	C	-4.0027	-2.84414	-0.5394
H	-5.31675	0.98252	2E-6	H	-3.69856	-3.88598	-0.49359
H	-5.30704	-0.56355	0.88397	H	-4.59796	-2.67417	-1.43908

H	-5.30704	-0.56354	-0.88397	H	-4.61891	-2.59958	0.32886
				Li	5.08916	-0.91445	0.73244
				Li	-5.11142	0.80713	0.75827
				O	5.64489	-2.61586	-0.13663
				H	5.21646	-2.8582	-0.96642
				H	6.58727	-2.71987	-0.31515
				O	6.8382	-0.34055	1.48064
				H	7.61824	-0.6073	0.97951
				H	6.98817	0.59192	1.67669
				O	-5.76441	2.55566	0.09341
				H	-6.27417	3.12735	0.6795
				O	-6.66044	-0.25791	1.41615
				H	-6.84074	-1.05306	0.90001
				H	-7.52085	0.16971	1.50132
				O	-3.88821	0.98559	2.32896
				O	3.8612	-1.15239	2.27467
				H	4.06957	-1.81394	2.94491
				H	2.93665	-1.32091	2.05304
				H	-2.9517	0.85405	2.13521
				H	-4.06522	0.38484	3.06266
				H	-5.11878	3.14635	-0.31295

NDI²⁻[Zn(H₂O)₅]NDI²⁻[Al(H₂O)₅]⁺

O	5.93326	0.62084	0.81653	O	5.86161	0.73976	0.42927
N	4.81021	-1.27914	0.14867	N	4.73724	-1.23892	0.06808
O	3.79542	-3.22501	-0.51087	O	3.71603	-3.25973	-0.28351
C	3.63376	0.82352	0.24999	C	3.50268	0.83138	0.15802
C	3.59018	2.22439	0.51324	C	3.44248	2.24341	0.30731
C	1.28346	-1.88348	-0.91494	C	1.12475	-2.02344	-0.46444
C	2.47545	-1.2416	-0.46097	C	2.34122	-1.31604	-0.22429
C	2.46469	0.15065	-0.18427	C	2.31439	0.09277	-0.06826
C	4.85409	0.09544	0.42747	C	4.76553	0.15252	0.2316
C	3.68029	-1.98497	-0.29321	C	3.584	-2.01084	-0.15573
H	4.50082	2.71852	0.83971	H	4.36736	2.78555	0.48239
H	1.32264	-2.9438	-1.1494	H	1.17218	-3.10009	-0.60274
O	-2.27717	0.37799	-1.14282	O	-2.50518	0.15558	-0.63479
N	-1.12536	2.2962	-0.5774	N	-1.35027	2.12713	-0.34327
O	-0.09661	4.25938	0.00313	O	-0.32731	4.14794	-0.0108
C	0.06444	0.21628	-0.75456	C	-0.14024	0.05055	-0.36307
C	0.11835	-1.18374	-1.05923	C	-0.07266	-1.37345	-0.53078
C	2.42948	2.93187	0.3618	C	2.24893	2.90979	0.22973
C	1.23188	2.27937	-0.06008	C	1.03907	2.1933	-0.00328
C	1.2446	0.89153	-0.33706	C	1.06368	0.78944	-0.14469
C	-1.15405	0.92624	-0.83558	C	-1.35173	0.74608	-0.42786
C	0.01548	3.01779	-0.20006	C	-0.20383	2.89879	-0.1087
H	-0.78039	-1.67191	-1.4255	H	-0.98713	-1.9221	-0.73025
H	2.39803	3.99863	0.56393	H	2.20346	3.98889	0.33976
C	-2.35614	3.06945	-0.69167	C	-2.58637	2.88282	-0.52568
H	-2.23636	3.85197	-1.44388	H	-2.42065	3.66649	-1.26503
H	-2.59095	3.54906	0.26073	H	-2.88707	3.35878	0.41111
H	-3.16515	2.40414	-0.98181	H	-3.37327	2.21713	-0.86888
C	6.02186	-2.06821	0.32488	C	5.99284	-1.97561	0.12544
H	6.81281	-1.41622	0.68456	H	6.8038	-1.26967	0.28012
H	6.32242	-2.5217	-0.62215	H	6.1527	-2.52238	-0.80604
H	5.8494	-2.87024	1.04567	H	5.97338	-2.69735	0.94485
O	-3.55366	0.8998	1.63881	O	-4.36015	0.54845	1.35421
H	-5.69489	0.19742	-0.25141	H	-5.93082	-0.17025	-1.04147
Zn	-3.2864	-0.83632	0.22986	Al	-3.77184	-0.85136	0.13924
H	-2.47118	-3.21115	-0.62276	H	-3.00414	-3.18674	-0.52648
O	-3.13403	-2.62892	-1.01827	O	-3.43855	-2.42225	-0.93229
O	-5.09215	-0.20818	-0.88898	O	-4.9902	-0.28746	-1.23901
H	-1.29468	-0.73976	1.95423	H	-3.07581	-2.00623	2.28249
H	-4.81389	-2.77401	1.25622	H	-5.53006	-2.66415	0.55657
O	-4.66475	-1.88582	1.60648	O	-5.23661	-1.83283	0.95749
H	-5.51837	-1.44439	1.50244	H	-6.03729	-1.37554	1.25532
O	-1.60845	-1.52756	1.48898	O	-2.64635	-1.65704	1.4869
H	-0.8816	-1.73956	0.87907	H	-1.83436	-1.21943	1.78442
H	-4.77454	0.53473	-1.42071	H	-4.71922	0.47212	-1.77652
H	-3.96212	-3.12086	-0.93746	H	-4.12282	-2.76726	-1.52395
H	-4.10166	1.53883	1.16375	H	-3.80938	1.34145	1.423
H	-4.12413	0.5832	2.35178	H	-4.59045	0.31276	2.26585

NDI²⁻[Al(OH)(H₂O)₄]

NDI neutral

O	5.72054	0.88354	0.67578	O	-3.52541	2.29203	0.00407
N	4.71737	-1.11722	0.1289	N	-3.52176	0.00416	-0.0063
O	3.8241	-3.15084	-0.43278	O	-3.53851	-2.26875	0.00528
C	3.38742	0.89371	0.22633	C	-1.40457	1.23202	0.00165
C	3.24991	2.29151	0.45005	C	-0.7006	2.42663	0.00327
C	2.25603	0.12177	-0.13247	C	-0.70059	-2.42289	0.00233
C	1.20322	-2.01437	-0.75503	C	-1.40285	-1.22738	0.00137
C	2.35912	-1.27437	-0.36708	C	-0.70898	0.00277	0.00104

C	4.67047	0.26373	0.36312	C	-2.87802	1.24531	3.49E-4
C	3.62396	-1.91996	-0.23908	C	-2.87387	-1.23179	7.35E-4
H	4.13286	2.86145	0.72495	H	-1.24463	3.36534	0.00408
H	1.31792	-3.07211	-0.97568	H	-1.24567	-3.36108	0.00275
O	-2.52397	-0.01637	-0.90252	O	3.53851	-2.26875	0.00529
N	-1.48324	1.99933	-0.50122	N	3.52176	0.00416	-0.0063
O	-0.55947	4.05451	-0.01632	O	3.52541	2.29203	0.00407
C	-0.16501	-0.00911	-0.60196	C	1.40285	-1.22738	0.00137
C	-0.01848	-1.41359	-0.86967	C	0.70059	-2.42289	0.00233
C	2.03443	2.90845	0.32329	C	0.7006	2.42663	0.00327
C	0.8772	2.15716	-0.03586	C	1.40457	1.23202	0.00165
C	0.98288	0.76743	-0.26081	C	0.70898	0.00277	0.00104
C	-1.40736	0.62822	-0.65893	C	2.87387	-1.23179	7.36E-4
C	-0.3902	2.81681	-0.17422	C	2.87802	1.24531	3.49E-4
H	-0.87761	-1.97414	-1.23145	H	1.24567	-3.36108	0.00275
H	1.92991	3.97535	0.49487	H	1.24463	3.36534	0.00408
C	-2.78769	2.62638	-0.69301	C	4.98203	-0.03719	-0.01086
H	-2.64829	3.70331	-0.71566	H	5.35673	0.98108	-0.04888
H	-3.46628	2.36161	0.12031	H	5.33151	-0.59459	-0.88061
H	-3.21786	2.29044	-1.63751	H	5.34284	-0.53102	0.89256
C	5.99446	-1.80623	0.2604	C	-4.98203	-0.03719	-0.01086
H	6.74164	-1.09239	0.59535	H	-5.35673	0.98108	-0.04887
H	6.29872	-2.23278	-0.6981	H	-5.34284	-0.53103	0.89256
H	5.91006	-2.61936	0.98367	H	-5.33152	-0.59458	-0.88061
O	-3.55351	0.44293	1.62639				
H	-5.89091	0.38528	-0.11285				
Al	-3.66596	-0.77734	0.32792				
H	-3.76552	-3.17333	-0.61952				
O	-3.91131	-2.27675	-0.9538				
O	-5.18039	0.01732	-0.6576				
H	-2.20337	-1.88798	2.06806				
H	-5.64161	-2.37758	0.96069				
O	-5.03082	-1.76605	1.39621				
H	-5.56444	-1.23284	2.00275				
O	-2.34748	-2.02366	1.11984				
H	-1.45693	-2.03561	0.72345				
H	-4.94058	0.71451	-1.28558				
H	-4.75441	-2.30254	-1.42861				
H	-3.60827	0.09725	2.52191				

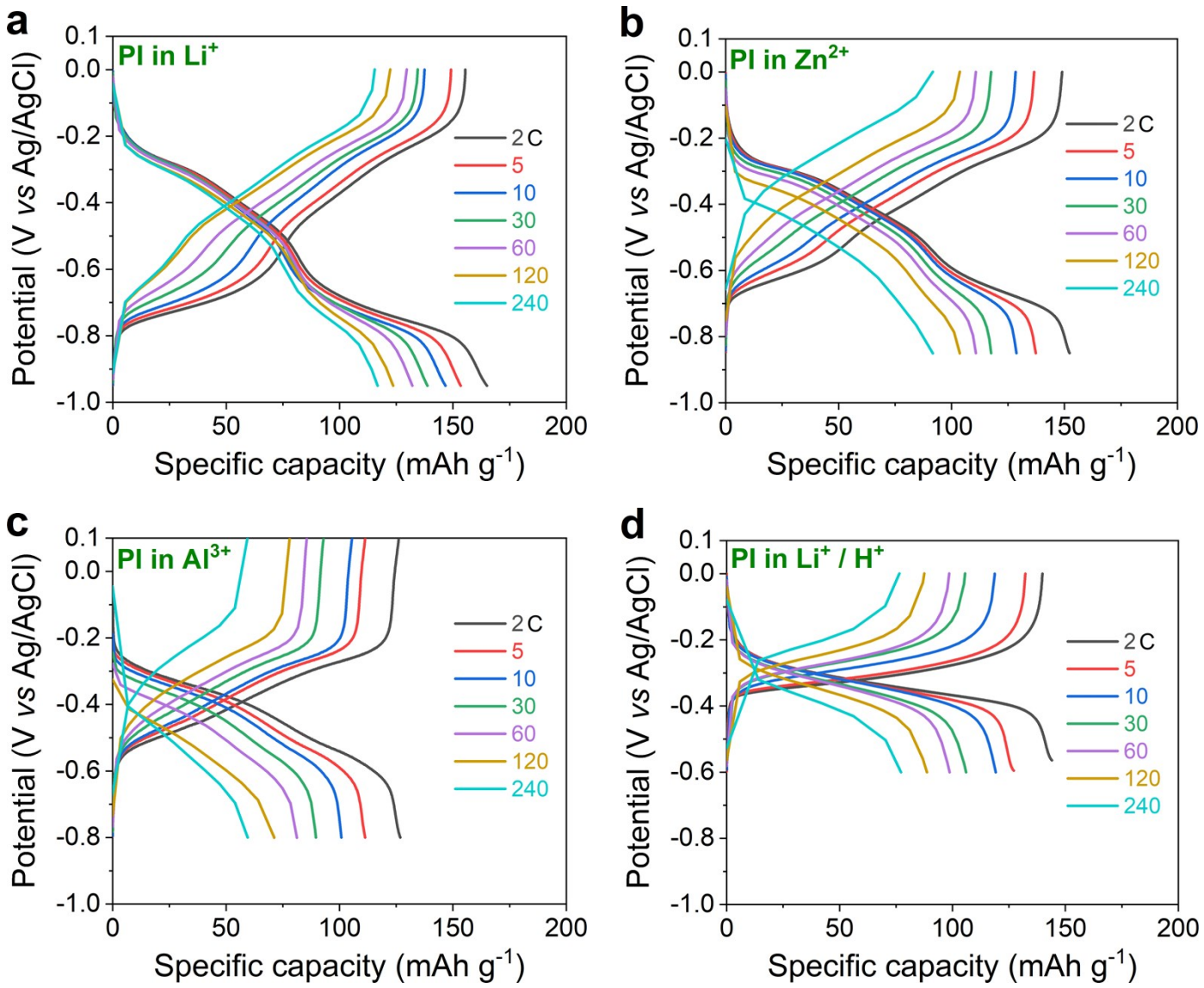


Figure S4. Rate performance of anode active-material, PI in aqueous electrolytes containing different charge carriers, carried out in a standard three electrode configuration. Representative galvanostatic capacity–potential profiles at various C-rates in Li^+ (a), Zn^{2+} (b), Al^{3+} (c), and Li^+/H^+ (d) containing aqueous electrolytes. $1\text{C} = 166 \text{ mA g}^{-1}$.

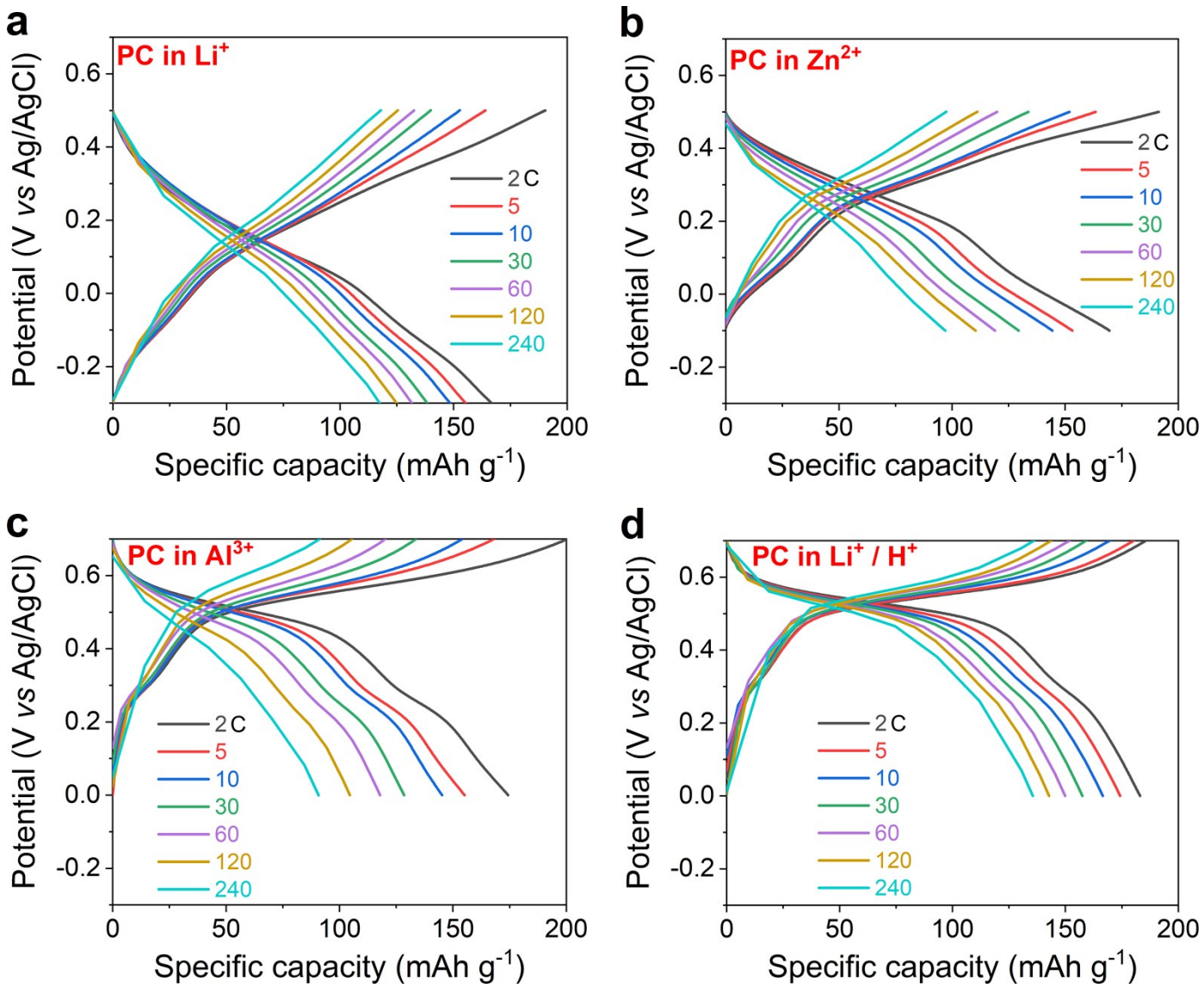


Figure S5. Rate performance of cathode active-material, PC in aqueous electrolytes containing different charge carriers, carried out in a standard three electrode configuration. Representative galvanostatic capacity–potential profiles at various C-rates in Li^+ (a), Zn^{2+} (b), Al^{3+} (c), and Li^+/H^+ (d) containing aqueous electrolytes. $1\text{C} = 180 \text{ mA g}^{-1}$.

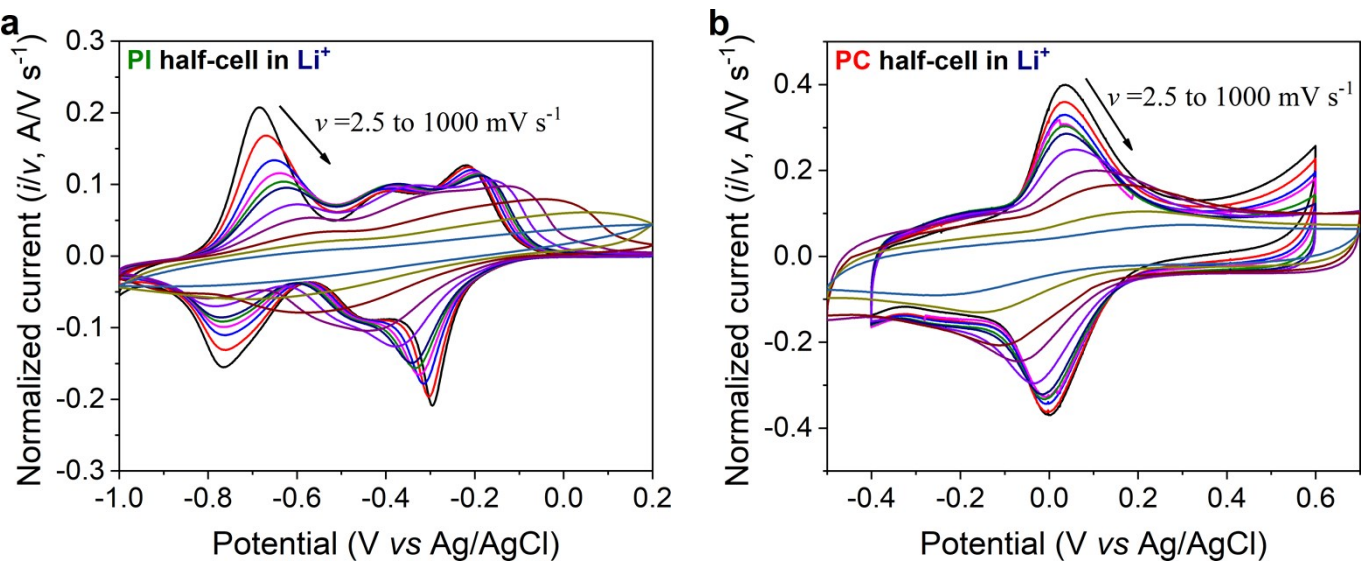


Figure S6. Kinetic analysis of PI and PC individual electrodes carried out in a standard three electrode configuration in Li^+ containing aqueous electrolyte. Cyclic voltammograms of PI (a), and PC (b) at different scan rates. The CVs are normalized by the scan rate to show the peak shift and decrease of the area enclosed with the scan rates.

Laviron formalism: A linear correlation between peak position (E_p) and scan rate (in logarithmic scale) was observed above $E_{\text{divergence}}$ (see Figure 4a, d in the main manuscript), and their correlation can be expressed by the following Laviron equations:

$$E_{p, \text{anodic}} = E^0 + \frac{2.303RT}{\alpha nF} \log v \quad (\text{Equation S1})$$

$$E_{p, \text{cathodic}} = E^0 - \frac{2.303RT}{(1-\alpha)nF} \log v \quad (\text{Equation S2})$$

$$\frac{\alpha}{(1-\alpha)} = \frac{\text{slope}_{\text{anodic}}}{\text{slope}_{\text{cathodic}}} \quad (\text{Equation S3})$$

where E_p is the peak position, E^0 is the formal redox potential, F is the Faraday constant, n is the number of electrons involved in the electrode reaction, R is the molar gas constant and T is the absolute temperature.

From the values of α and $E_{\text{divergence}}$, k^0 was evaluated as follows:

$$k^0 = \frac{2.303 \alpha nF E_{\text{divergence}}}{RT}$$

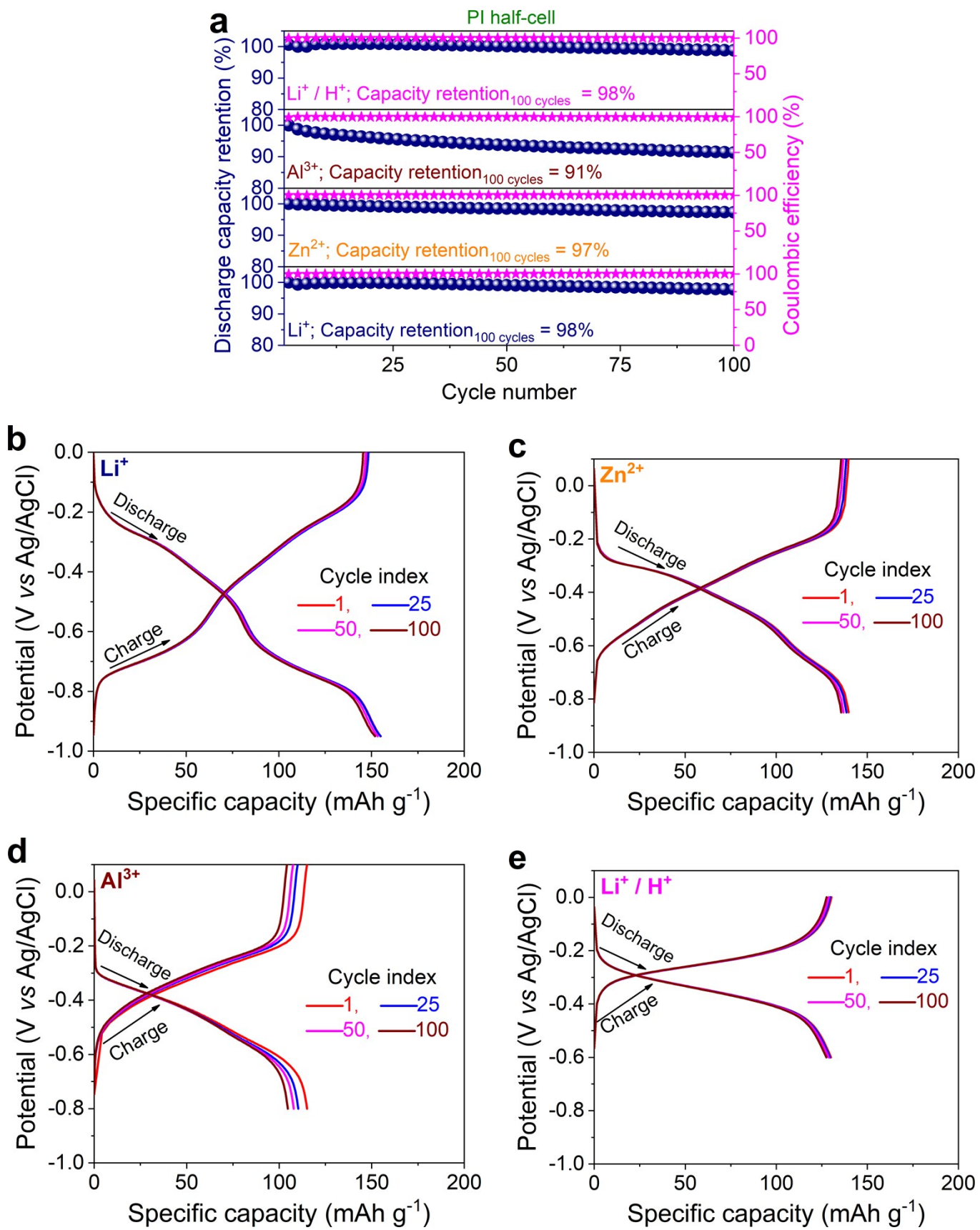


Figure S7. Cyclic performance of anode active-material, PI in aqueous electrolytes containing different charge carriers, carried out in a standard three electrode configuration. a) Discharge capacities and Coulombic efficiencies measured at 10C, and b)

Representative galvanostatic capacity–potential profiles over 100 GCD cycles in Li^+ (b), Zn^{2+} (c), Al^{3+} (d), and Li^+/H^+ (e) containing aqueous electrolytes. 1C = 166 mA g⁻¹.

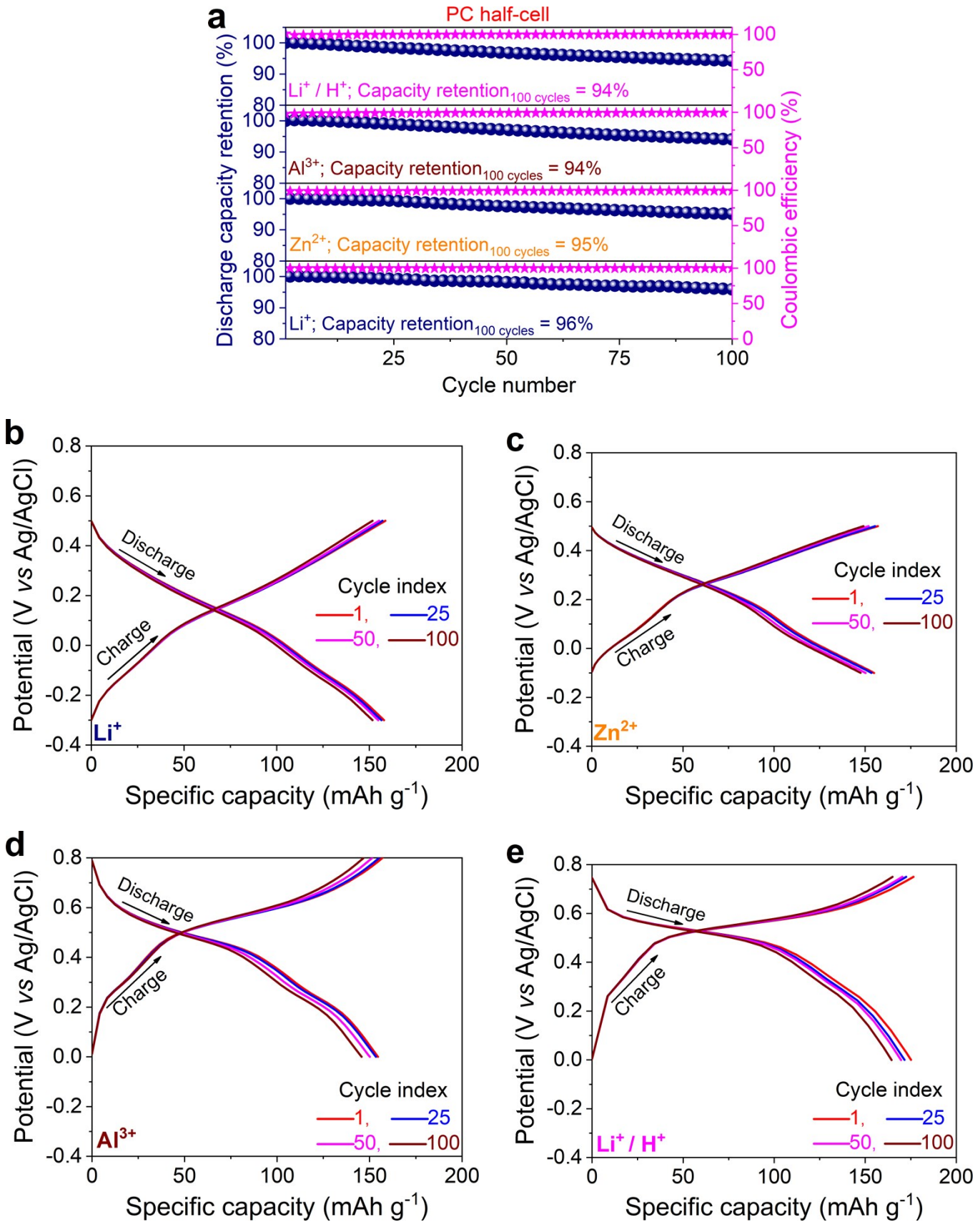


Figure S8. Cyclic performance of cathode active-material, PC in aqueous electrolytes containing different charge carriers, carried out in a standard three electrode configuration. a) Discharge capacities and Coulombic efficiencies measured at 10C, and b)

Representative galvanostatic capacity–potential profiles over 100 GCD cycles in Li^+ (b), Zn^{2+} (c), Al^{3+} (d), and Li^+/H^+ (e) containing aqueous electrolytes. $1\text{C} = 180 \text{ mA g}^{-1}$.

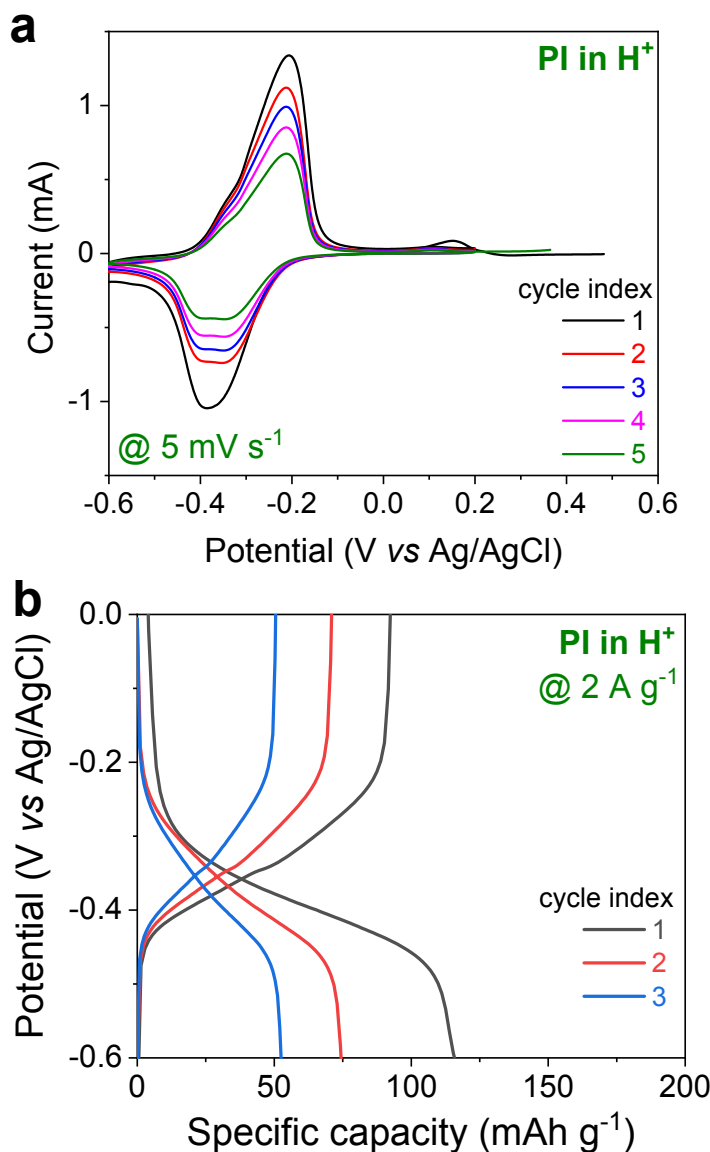


Figure S9. Electrochemical performance of PI in $0.25 \text{ M H}_2\text{SO}_4$ aqueous electrolyte, carried out in a standard three electrode configuration. a) CVs at 5 mV s^{-1} , and b) galvanostatic capacity–potential profiles at 2 A g^{-1} .

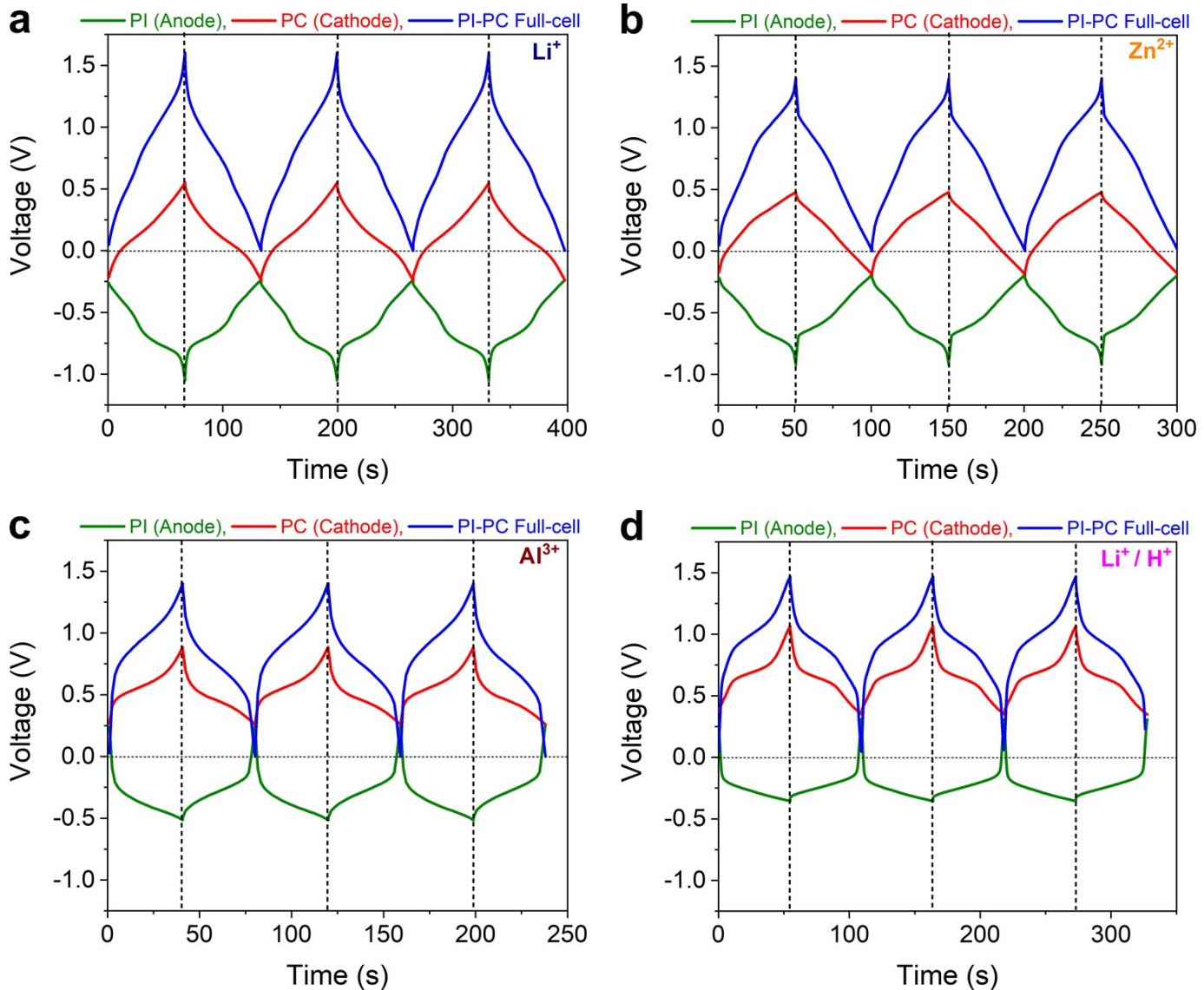


Figure S10. Validation of mass balance between anode- and cathode-electrode materials in order to fabricate an optimal full-cell. The real-time evolution of individual voltages of PI anode, PC cathode and PI-PC full-cells at a current density of 10 A g^{-1} in Li^+ (a), Zn^{2+} (b), Al^{3+} (c), and Li^+ / H^+ (d) containing aqueous electrolytes.

Figure S10 shows that PI and PC customarily work in opposite potential directions, leading to the maximum operating cell voltage window that is consistent with the potential difference between the cathode and the anode partners observed in the three-electrode systems. It can be also observed from Figure S10 that both PI anode and PC cathode concomitantly arrive to their limiting lower and upper cut-off potentials, respectively, when the full-cell reaches the corresponding maximum voltage, without the sacrifice of capacity, confirming an acceptable mass balancing.

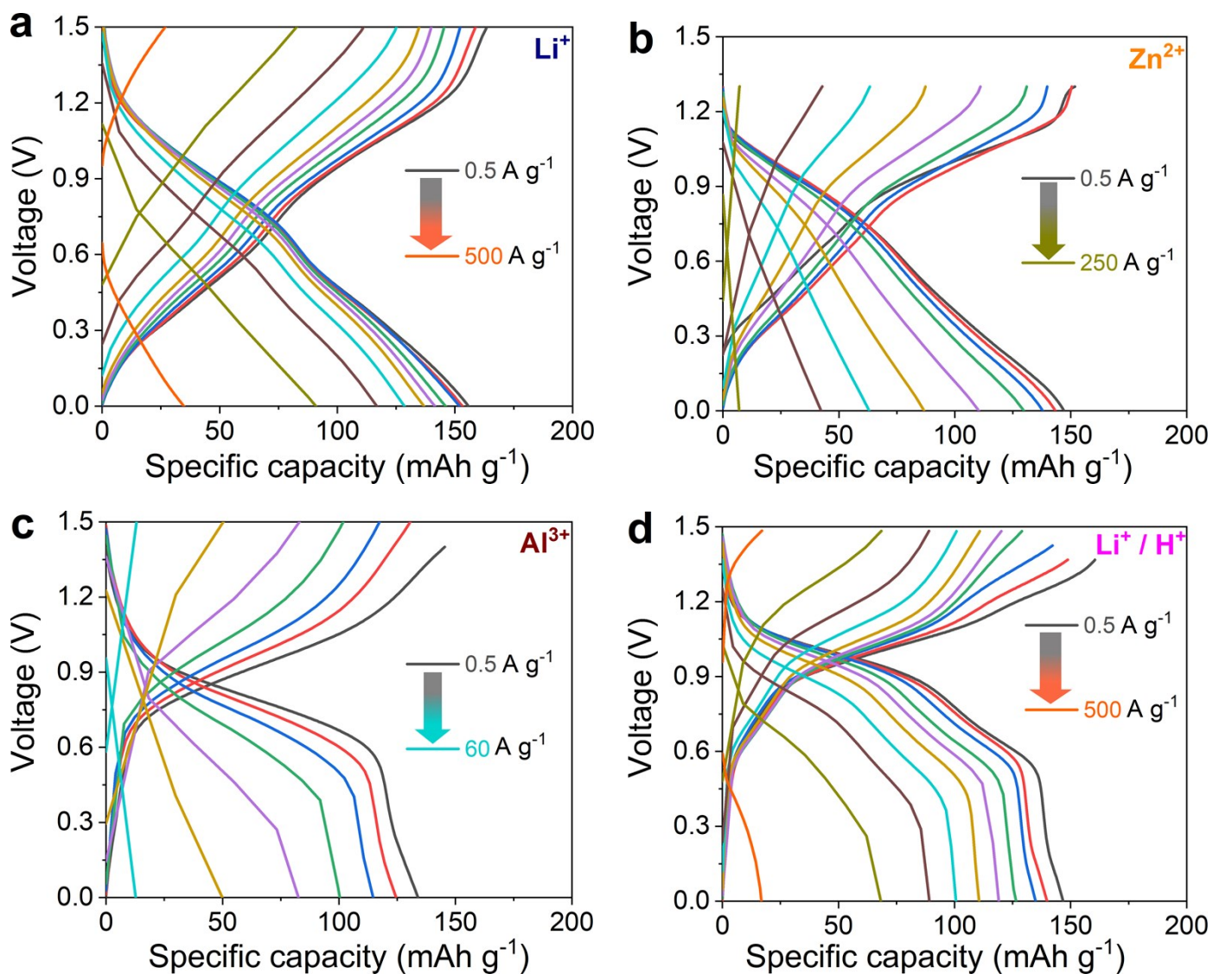


Figure S11. Rate performance of PI–PC full-cells in aqueous electrolytes containing different charge carriers. a–d) Representative galvanostatic capacity–voltage profiles at various current densities in Li⁺ (a), Zn²⁺ (b), Al³⁺ (c), and Li⁺/H⁺ (d) containing aqueous electrolytes. The capacities and current densities were based on the PI component of the full-cell.

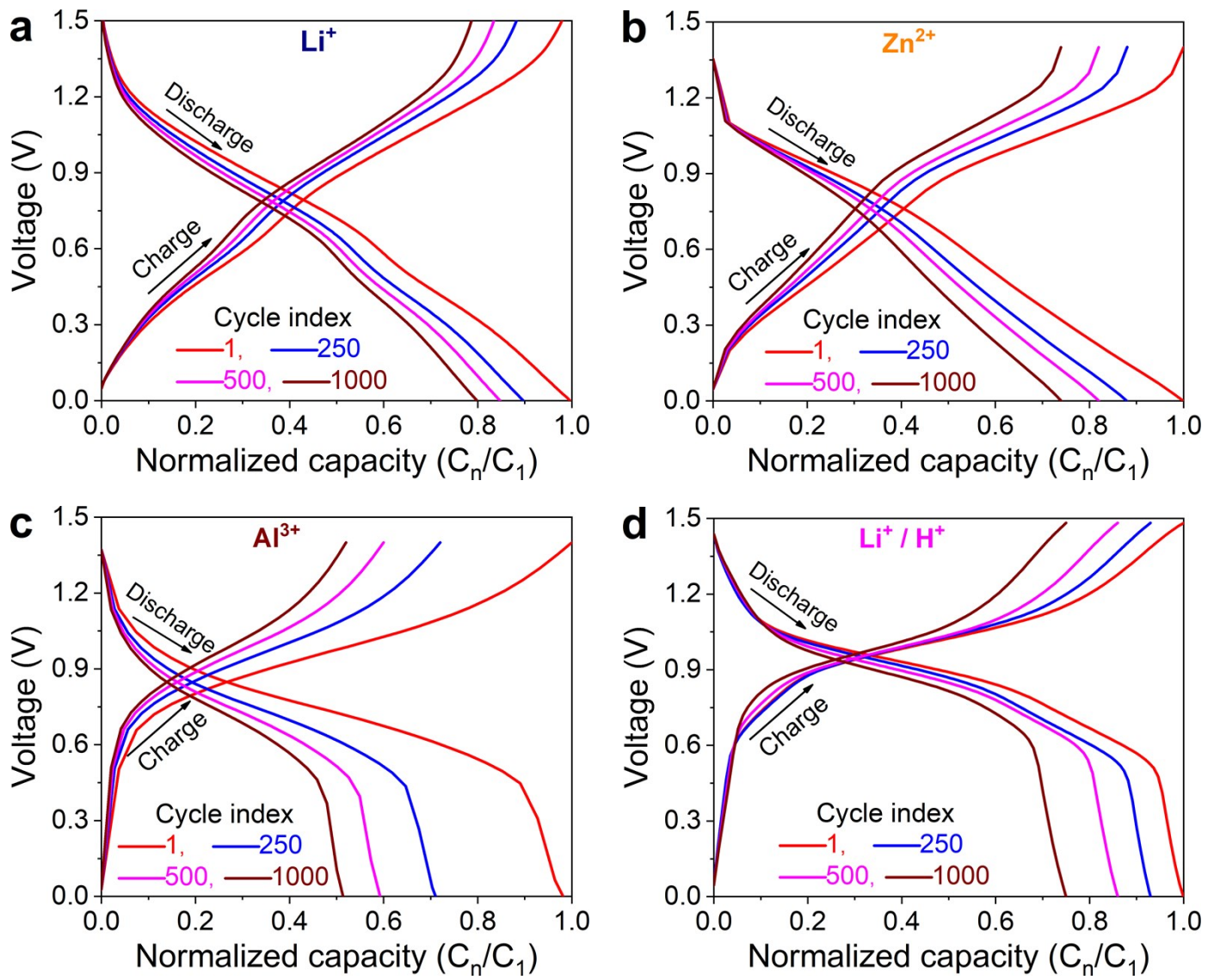


Figure S12. Cyclic performance of PI-PC full-cells in aqueous electrolytes containing different charge carriers. a–d) Representative galvanostatic normalized capacity–voltage profiles over 1000 GCD cycles in Li^+ (a), Zn^{2+} (b), Al^{3+} (c), and Li^+/H^+ (d) containing aqueous electrolytes.

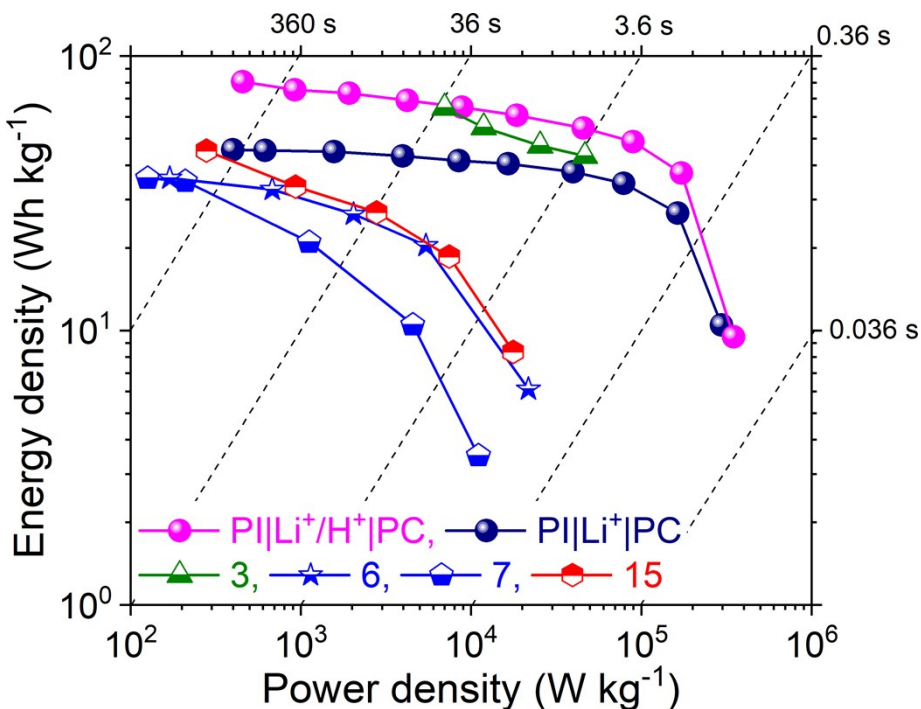


Figure S13. Comparing PI|Li⁺|PC and PI|Li⁺/H⁺|PC cell performance in the Ragone plot with the state-of-the-art all-polymer aqueous stationary batteries. The gravimetric energy/power density was evaluated based on the total mass of the anode, cathode and consumed salt (charge carriers in the electrolyte).

Supplementary References

- 1 N. Chikushi, H. Yamada, K. Oyaizu and H. Nishide, *Sci. China Chem.*, 2012, **55**, 822–829.
- 2 K. Sato, R. Katagiri, N. Chikushi, S. Lee, K. Oyaizu, J.-S. Lee and H. Nishide, *Chem. Lett.*, 2017, **46**, 693–694.
- 3 N. Sano, W. Tomita, S. Hara, C.-M. Min, J.-S. Lee, K. Oyaizu and H. Nishide, *ACS Appl. Mater. Interfaces*, 2013, **5**, 1355–1361.
- 4 K. Hatakeyama-Sato, H. Wakamatsu, K. Yamagishi, T. Fujie, S. Takeoka, K. Oyaizu and H. Nishide, *Small*, 2019, **15**, 1805296.
- 5 X. Dong, H. Yu, Y. Ma, J. L. Bao, D. G. Truhlar, Y. Wang and Y. Xia, *Chem. - A Eur. J.*, 2017, **23**, 2560–2565.
- 6 Y. Zhang, Y. An, B. Yin, J. Jiang, S. Dong, H. Dou and X. Zhang, *J. Mater. Chem. A*, 2019, **7**, 11314–11320.
- 7 H. Long, W. Zeng, H. Wang, M. Qian, Y. Liang and Z. Wang, *Adv. Sci.*, 2018, **5**, 1700634.
- 8 R. Emanuelsson, M. Sterby, M. Strømme and M. Sjödin, *J. Am. Chem. Soc.*, 2017, **139**, 4828–4834.
- 9 G. Hernández, N. Casado, A. M. Zamarayeva, J. K. Duey, M. Armand, A. C. Arias and D. Mecerreyes, *ACS Appl. Energy Mater.*, 2018, **1**, 7199–7205.
- 10 Y. Zhang, Y. An, L. Wu, H. Chen, Z. Li, H. Dou, V. Murugadoss, J. Fan, X. Zhang, X. Mai and Z. Guo, *J. Mater. Chem. A*, 2019, **7**, 19668–19675.

- 11 N. Patil, A. Mavrandonakis, C. Jérôme, C. Detrembleur, J. Palma and R. Marcilla, *ACS Appl. Energy Mater.*, 2019, **2**, 3035–3041.
- 12 Y. Zhao and D. G. Truhlar, *Acc. Chem. Res.*, 2008, **41**, 157–167.
- 13 K. L. Schuchardt, B. T. Didier, T. Elsethagen, L. Sun, V. Gurumoorthi, J. Chase, J. Li and T. L. Windus, *J. Chem. Inf. Model.*, 2007, **47**, 1045–1052.
- 14 A. V Marenich, C. J. Cramer and D. G. Truhlar, *J. Phys. Chem. B*, 2009, **113**, 6378–6396.
- 15 M. J. Frisch, G. W. Trucks, H. B. Schlegel, G. E. Scuseria, M. A. Robb, J. R. Cheeseman, G. Scalmani, V. Barone, G. A. Petersson, H. Nakatsuji, X. Li, M. Caricato, A. V Marenich, J. Bloino, B. G. Janesko, R. Gomperts, B. Mennucci, H. P. Hratchian, J. V Ortiz, A. F. Izmaylov, J. L. Sonnenberg, D. Williams-Young, F. Ding, F. Lipparini, F. Egidi, J. Goings, B. Peng, A. Petrone, T. Henderson, D. Ranasinghe, V. G. Zakrzewski, J. Gao, N. Rega, G. Zheng, W. Liang, M. Hada, M. Ehara, K. Toyota, R. Fukuda, J. Hasegawa, M. Ishida, T. Nakajima, Y. Honda, O. Kitao, H. Nakai, T. Vreven, K. Throssell, J. A. Montgomery, J. E. P. Jr., F. Ogliaro, M. J. Bearpark, J. J. Heyd, E. N. Brothers, K. N. Kudin, V. N. Staroverov, T. A. Keith, R. Kobayashi, J. Normand, K. Raghavachari, A. P. Rendell, J. C. Burant, S. S. Iyengar, J. Tomasi, M. Cossi, J. M. Millam, M. Klene, C. Adamo, R. Cammi, J. W. Ochterski, R. L. Martin, K. Morokuma, O. Farkas, J. B. Foresman and D. J. Fox, 2016.